

Hydrogenated amorphous silicon carbide deposition using electron cyclotron resonance chemical vapor deposition under high microwave power and strong hydrogen dilution

K. Chew, Rusli,^{a)} S. F. Yoon, J. Ahn, and V. Ligatchev

Microelectronics Division, School of Electrical and Electronic Engineering, Nanyang Technological University, Singapore 639798, Republic of Singapore

E. J. Teo, T. Osipowicz, and F. Watt

Research Centre for Nuclear Microscope, Physics Department, National University of Singapore, 10 Kent Ridge Crescent, Singapore 119260

(Received 24 April 2002; accepted for publication 21 June 2002)

We have investigated the growth of $a\text{-Si}_{1-x}\text{C}_x\text{:H}$ using the electron cyclotron resonance chemical vapor deposition (ECR-CVD) technique, under the conditions of high microwave power and strong hydrogen (H_2) dilution. The microwave power used is 900 W and a gas mixture of CH_4 and SiH_4 diluted in H_2 is varied to give carbon (C) fractions x ranging from 0 to 1. We aim to understand the effects of these deposition conditions on the characteristics of ECR-CVD grown $a\text{-Si}_{1-x}\text{C}_x\text{:H}$ films at different x . Their microstructure and optical properties are investigated using infrared absorption, Raman scattering, UV-visible spectrophotometry, and photothermal deflection spectroscopy. Information on the atomic fraction x is obtained with Rutherford backscattering spectrometry. The B parameter in the Tauc relation is found to decrease and the Urbach energy E_u increase with x , which are indicative of a higher degree of disorder with C incorporation. At intermediate x , the presence of Si—C bonds can be clearly seen from the IR absorption and Raman scattering results. The T peak around 1200 cm^{-1} is observed in the Raman spectra of the C-rich samples, with a redshift noted at increasing x . This suggests an increased presence of sp^3 C—C bonds in these films, which is attributed to the high microwave power and strong H_2 dilution that enhance C sp^3 bonding and indirectly limit the number of C sp^2 sites. This accounts for the large E_{04} gaps of more than 3.2 eV observed in such films, which are nearly saturated at large x , instead of exhibiting a maximum at an intermediate x as are commonly reported. Blue photoluminescence (PL) is observed, and the PL peak energies (E_{PL}) are correlated to the E_{04} gap. The full width at half maximum of the PL are also correlated to the Urbach energy E_u . These results support that the PL broadening is attributed to the disorder broadening arising from the broad band tails. © 2002 American Institute of Physics. [DOI: 10.1063/1.1500418]

I. INTRODUCTION

There are several technological advantages in alloying C with hydrogenated amorphous silicon ($a\text{-Si:H}$) to form hydrogenated amorphous silicon carbide ($a\text{-Si}_{1-x}\text{C}_x\text{:H}$). Most importantly, carbon alloying increases the band gap, while retains its ability to be doped n and p type. This variability renders $a\text{-Si}_{1-x}\text{C}_x\text{:H}$ potentially attractive for electronic applications, such as solar cells, optoelectronic devices, and high-temperature engineering materials.¹⁻³

In this study, we investigate $a\text{-Si}_{1-x}\text{C}_x\text{:H}$ films grown with the electron cyclotron resonance chemical vapor deposition (ECR-CVD) technique, which has the unique characteristics of a high plasma density, high electron temperature, and controllable ion energy that can be independent of the degree of plasma ionization.^{4,5} In our previous study on the effect of microwave power on ECR-CVD grown $a\text{-Si}_{1-x}\text{C}_x\text{:H}$, it was noted that the Si—C infrared absorption band at $\sim 800\text{ cm}^{-1}$ can only be clearly seen for films deposited at high microwave powers beyond 800 W.⁶ On the effect

of hydrogen incorporation in $a\text{-Si}_{1-x}\text{C}_x\text{:H}$, previous reports have shown that stronger hydrogen dilution in the gas mixture will lead to films with lower defect densities and smaller Urbach energies, and result in improved optoelectronic properties, such as enhanced photoconductivity.^{7,8} Based on these considerations, it is interesting to study $a\text{-Si}_{1-x}\text{C}_x\text{:H}$ films with different carbon fractions ranging from $x=0$ ($a\text{-Si:H}$) to $x=1$ ($a\text{-C:H}$), deposited under a combination of high microwave power and strong hydrogen dilution. Our focus will be on the effect of these deposition conditions on the structural, optical, and luminescence characteristics of these films. The films are characterized using the Rutherford backscattering spectrometry (RBS), photothermal deflection spectroscopy (PDS), UV-visible (UV-VIS) spectrophotometry, infrared absorption, Raman scattering, and room-temperature photoluminescence (PL).

II. EXPERIMENTS

The schematic diagram of the ECR-CVD system used can be found elsewhere.⁵ The microwave power at 2.45 GHz was set to 900 W, and the upper and lower magnetic current

^{a)}Electronic mail: erusli@ntu.edu.sg

were kept at 120 A and 100 A, respectively. The hydrogen (H_2) flow rate was kept at 100 sccm while those of silane (SiH_4 , 10% diluted in H_2) to methane (CH_4) were varied (20/0, 20/0.5, 45/2, 35/2, 19/2, 2/2, and 0/2 sccm) to produce films with varying C fraction from $x=0$ to 1. The deposition pressure was maintained at 20 mT and there was no intentional heating applied. For ease of discussion, the films are named according to their C contents, e.g., SC69 denotes the sample with $x=0.69$.

The C fractions x of the films were deduced using RBS, with 2 MeV H^+ . The surface barrier detector was mounted at 20° scattering angle to detect the backscattered particles. The transmittance and reflectance spectra were measured using a dual beam Perkin-Elmer Lambda 16 UV-VIS spectrophotometer. The PDS measurements were performed using a conventional setup similar to that found in Ref. 9. The PDS spectra obtained were normalized and matched to the absorption spectra at higher energy deduced from UV-VIS spectrophotometry. Infrared absorption was measured with the Perkin-Elmer 2000 Fourier transform infrared (FTIR) spectrophotometer to study the bonding configuration in $\alpha-Si_{1-x}C_x:H$. The Raman spectra were measured using the Renishaw micro-Raman System 2000 spectrometer. Two excitation sources in the visible and UV range were used. The visible excitation source (632.8 nm line from a He-Ne laser) was used for the Si-rich samples as no Raman signal could be observed when excited with the UV source, attributed to the shallow penetration depth as a result of the high photon energy compared to the optical gaps of these films. On the other hand, the C-rich samples exhibited strong room-temperature PL under visible excitation, hence, the Raman measurements for such samples were excited using a UV source at 244 nm derived from a frequency-doubled Ar^+ laser (Coherent 90C FreD series). The scattered light was collected in a back scattering configuration with a charge coupled device camera, and multilayer dielectric filters were used to remove Rayleigh scattering light. The incident power on the samples was approximately 1.5 mW. For the UV Raman, the samples were rotated during measurement to prevent the high photon energy from damaging the film. The spectral resolution (half width, half maximum) for visible and UV spectrometers are 2.0 and 4.0 cm^{-1} respectively. PL was measured at room temperature, excited using the 363.8 nm UV line from an argon-ion laser. The PL was detected by a water-cooled photomultiplier tube (PMT), based on the single-photon counting technique. The PL spectra are corrected for the combined response of the PMT and the monochromator.

III. RESULTS AND DISCUSSION

The FTIR transmission spectra of the films are shown in Fig. 1. The 640 cm^{-1} peak seen for $x \leq 0.36$ can be assigned to $Si-H_n$ wagging or rocking mode.^{10,11} It gradually diminishes with increasing x , before disappearing in sample SC69 and beyond. The band observed at 790 cm^{-1} appears weak at low x , but becomes prominent in SC69, and subsequently vanishes for larger x . This band can be assigned to $Si-C$ stretching,¹² $Si-CH_3$ rocking/wagging, or $Si-CH_2-Si$

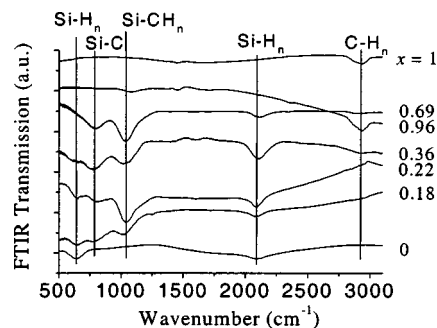


FIG. 1. The FTIR spectra of $\alpha-Si_{1-x}C_x:H$ at varying carbon fraction x . These are displaced vertically for clarity.

stretching mode.^{11,13} As the band has been shown to have similar strength in sputtered alloys prepared with and without hydrogen, it is therefore assigned to $Si-C$ stretching mode for our films.¹⁴ Previously, we have shown that the $Si-C$ stretching band appears only in samples grown at high microwave powers ($\geq 800\text{ W}$), owing to the stronger etching effect of H at these microwave powers that helps to etch away weakly bonded $Si-Si$ bonds and promotes the growth of $Si-C$ tetrahedral network.⁶ The observation of $Si-C$ bonds in these samples deposited under high microwave power further confirms the findings. The band at around $1020\text{ to }1040\text{ cm}^{-1}$ can be assigned to the vibrational mode of $C-H_n$ group to which silicon atoms are attached [$Si-(CH_n)$].^{11,15} Similar to the $Si-C$ bond, this mode peaks at an intermediate x of 0.69, due to the fact that it involves the bonding of both Si and C. The band located at approximately 2100 cm^{-1} can be due to a combination of $Si-H_n$ stretching ($n=1,2,3$) modes.^{10,12} It can be seen in samples with C contents up to $x=0.69$. Contrary to the expectation that this band peaks at $x=0$, as for the 640 cm^{-1} peak, its strength is strongest at intermediate x . It is known that the 2100 cm^{-1} peak, when accompanied by the absorption at $800-900\text{ cm}^{-1}$, is mainly attributed to $Si=H_2$ and $Si\equiv H_3$, whereas the 640 cm^{-1} peak is primarily associated with $Si-H$.¹⁶ However, as the 2100 cm^{-1} peak observed in our samples is not accompanied by the modes at $800-900\text{ cm}^{-1}$, it is assumed that this peak is associated with $Si-H$. Indeed, it has been suggested that $Si-H$ can also give rise to the absorption at 2100 cm^{-1} , when it is in a different environment.¹⁶ We believe that this is indeed the case in our films, whereby with changing microstructures in the presence of increasing C incorporation, this peak at 2100 cm^{-1} appears. It is also noted that the peak shifts slightly toward higher wave numbers with increasing x , which can be attributed to the increase in the sum of electronegativity around Si atoms when more C are included into the microstructure, in good agreement with other reports.^{15,17}

With increasing C incorporation, the sp^3 $C-H_n$ ($n=1,2,3$) stretching modes around 2940 cm^{-1} starts to appear in SC36,¹³ and can be clearly seen in SC96 and SC100. One possible reason that the band appears only when there is a high C concentration in the films could be that the absorption of $C-H_n$ stretching modes are lower than that of $Si-H_n$ modes by one order of magnitude.¹⁵ Another possible reason is the strong H_2 dilution, which promotes the transformation

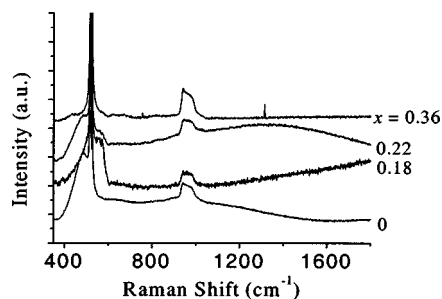


FIG. 2. Raman spectra of Si-rich $a\text{-Si}_{1-x}\text{C}_x\text{:H}$ excited using a visible source (632.8 nm).

of polymericlike $(\text{CH}_2)_n$ chains into diamondlike (sp^3 sites of C—C bonding) networks by etching away weakly bonded C—H sites and sp^2 C—C bonds. This results in an increased C incorporation and a reduced number of C— H_n groups.⁷ The sp^2 C— H_n bands expected above 3000 cm^{-1} are not found in our films.¹⁷ This may be because H is preferentially bonded to sp^3 instead of sp^2 sites of C, as suggested by the results obtained from nuclear magnetic resonance studies on plasma deposited carbon—hydrogen alloys.¹⁸

The Raman spectra for the Si-rich $a\text{-Si}_{1-x}\text{C}_x\text{:H}$ under visible excitation are shown in Fig. 2. The amorphous Si—Si vibrational mode and the Si substrate signals at around 480 and 520 cm^{-1} , respectively are clearly seen in all the spectra. The broad peaks at around 950 cm^{-1} are the associated second-order Raman scattering signals. A band of weak signals around 650 to 1000 cm^{-1} , attributed to Si—C bonds, can be seen for SC36. This is consistent with what has been found from the FTIR results. The D and G bands associated with graphite-like and disordered clusters for sp^2 coordinated C, expected at ~ 1350 and 1550 cm^{-1} , respectively,¹⁹ are not detected in the Si-rich samples.

The Raman spectra for the C-rich $a\text{-Si}_{1-x}\text{C}_x\text{:H}$ under UV excitation are shown in Fig. 3. The G peak and the D peak are clearly seen in all the three samples. The G peak is shifted to lower frequency, and the ratio of the D to G peak intensity (I_D/I_G) is decreased with increasing x . In the Raman study of hydrogenated amorphous carbon ($a\text{-C:H}$) films, Ferrari *et al.*²⁰ found that there is a strong correlation between the G peak position and I_D/I_G with the sp^3 content, with both of them decreasing at increasing sp^3 fraction.²⁰

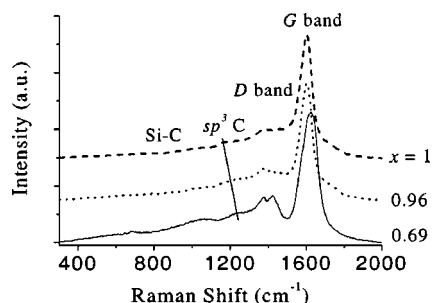


FIG. 3. Raman spectra of C-rich $a\text{-Si}_{1-x}\text{C}_x\text{:H}$ excited using an UV source (244 nm). The line serves as a guide for the eye for the energy shift of the T peak that is assigned to sp^3 C.

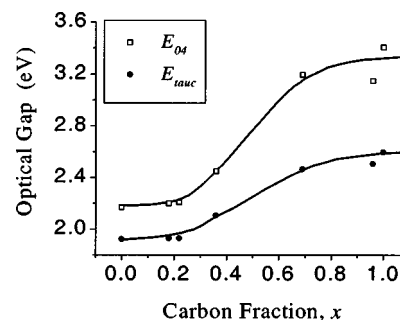


FIG. 4. Variation of the Tauc gap E_{tauc} and E_{04} with carbon fraction x .

Thus, the Raman scattering results in Fig. 3 suggest an enhancement of $C\text{ }sp^3$ bonding at larger x . This might be due to the high microwave power utilized that encourages their formation in C-rich samples. It is noted that boron doped $a\text{-Si}_{1-x}\text{C}_x\text{:H}$ deposited under high microwave powers ($\geq 800\text{ W}$) have also shown a diamondlike phase in the C bonding.²¹ Besides exciting the $\pi-\pi^*$ transitions, the higher excitation energy of UV Raman ($\sim 5.1\text{ eV}$) can also excite the σ states of both the sp^2 and sp^3 sites. This leads to the observation of the T peak by Gilkes *et al.*²² in their tetrahedral amorphous carbon ($ta\text{-C}$) films around 1200 cm^{-1} that can be assigned to the bond-stretching modes of sp^3 C—C sites. It is further shown that there is a redshift of the peak position with increasing sp^3 fraction. The T peak is also observed in our C-rich samples, with a redshift noted at increasing x . This suggests an increased presence of sp^3 C—C bonds in the C-rich films, consistent with the changes observed for the D and G peaks. The 650 cm^{-1} to 1050 cm^{-1} bands seen in the SC69 spectrum could be attributed to Si—C bonds, in good agreement with the deduction from the IR absorption results, confirming the presence of such bonds in the samples with an intermediate x .

From the absorption spectra, the optical band gap of $a\text{-Si}_{1-x}\text{C}_x\text{:H}$ can be found. The Tauc gap E_{tauc} is obtained through the Tauc's relation $(\alpha h\nu)^{1/2} = B(h\nu - E_{\text{tauc}})$, where α is the absorption coefficient, B is the joint optical density of states, and $h\nu$ is the photon energy. The E_{04} gap, defined as the energy at which $\alpha = 10^4\text{ cm}^{-1}$, is also used for comparison. These are plotted in Fig. 4 as a function of x . It is found that E_{tauc} increases with C incorporation before it nearly saturates when x reaches 0.69. E_{04} also shows the same increasing trend as E_{tauc} , though consistently higher by approximately 0.3 eV for the Si-rich and 0.7 eV for the C-rich samples. The reason behind the increase in the band gap with x is elucidated by calculations performed by Robertson for crystalline silicon carbide ($c\text{-SiC}$), which can serve as a first approximation to its amorphous counterpart.²³ Moving the C concentration away from $x = 0.5$ will give rise to chemical disorder which allows for homonuclear bonds. In our Si-rich $a\text{-Si}_{1-x}\text{C}_x\text{:H}$, as evidenced by the FTIR and Raman spectra, a large number of Si—Si bonds are present. Their σ -like and σ^* -like states are situated at 0.5 eV below the valence band edge (E_v) and 1.7 eV above the conduction band edge (E_c) of $c\text{-SiC}$, respectively.²³ The large number of Si—Si bonds prompts the Si—Si σ states to broaden into a band, which raises E_v closer to E_c and thus lowers the en-

ergy gap. With C incorporation, the Si—Si bonds are gradually replaced by the stronger Si—C bonds due to the tendency for higher local chemical ordering in the microstructure,¹² and so opens up the energy gap. Indeed, the FTIR results shown in Fig. 1 confirmed that the strength of the Si—C peak grows with the optical gap. When x continues to increase such that the samples become C rich, the optical gap will now be determined by the sp^2 and sp^3 C—C bonding. The former is weaker than the Si—C bonds and its π and π^* states are closer in energy and nearer to the band edges. As a result, any further increase in the optical gap will be limited, or it might even decrease²³ if there is a substantial amount of C sp^2 bonding. This will lead to a maximum optical gap in a -Si_{1-x}C_x:H at an intermediate x , when the band edges cross from Si-like to C-like, as are commonly reported.²⁴ On the other hand, if sp^3 C—C dominates the microstructures, there can be a continuous increase in the optical gap with x for a -Si_{1-x}C_x:H, even at large x .¹⁰ Our UV Raman results (Fig. 3) reveal the presence of both sp^2 and sp^3 C—C bonding in the C-rich samples, with an enhancement of the latter at increasing x . This accounts for the optical gap observed that exhibits a slight increase, instead of a decrease, at larger x .

In general, the samples exhibit high optical gaps across x . This can be attributed to the high microwave power and strong H dilution used in the experiment. The former enhances the dissociation of H₂, and the latter results in a high density of H radicals in the plasma. It has been reported that the optical gaps of a -Si_{1-x}C_x:H deposited with strong H dilution are larger compared to those that are undiluted.⁷ In Si-rich a -Si_{1-x}C_x:H, H tends to passivate (Si) dangling bonds, resulting in a lattice of Si—H sites, or break strained Si—Si bonds, to form stronger Si—Si bonds. This recedes the valence band, leading to a sharper and more abrupt valence band edge, and thus increases the optical gap. In C-rich a -Si_{1-x}C_x:H, H promotes C sp^3 over sp^2 bonding, thus indirectly reducing the sp^2 fraction, and accounts for the large band gap observed. In both cases, the optical gaps are widened. E_{04} gaps of more than 3.2 eV have been obtained under these deposition conditions for our samples at large x .

The extent of disorder-induced localization of states near the band edges, which leads to tail states extending into the gap can be measured by the Urbach energy E_u using the equation $\alpha = \alpha_0 \exp(h\nu/E_u)$, where α_0 is a pre-exponential factor. The B parameter in the Tauc equation and E_u are shown in Fig. 5. For $x \leq 0.36$, the B values are quite large, in agreement with the values reported for Si rich a -Si_{1-x}C_x:H.^{13,25} This is attributed to a Si dominated microstructure and a mostly sp^3 bonding environment, as can be seen from the FTIR and Raman results. Compared to high-quality a -Si:H and Si-rich a -Si_{1-x}C_x:H, these Si-rich samples show slightly lower B and higher E_u , probably due to more configurational and structural arrangement possibilities for C bonding, as a result of the strong dissociation of CH₄ under high microwave power deposition. With C incorporation, the C related bonding configurations become more prominent. Therefore, the microstructure will be more disordered owing to the different bond lengths and bond strengths of Si and C, as elucidated by the evolution of B and E_u .

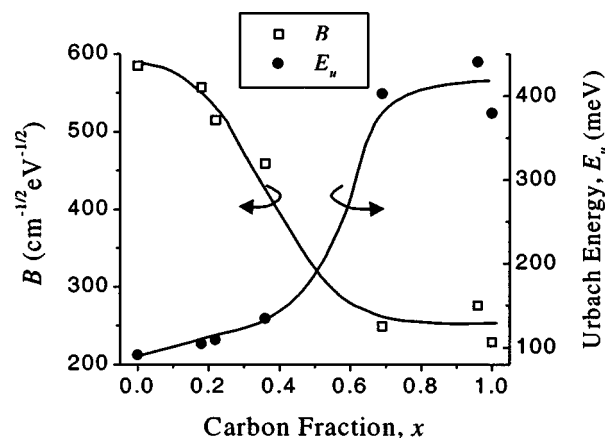


FIG. 5. Variation of the Tauc B parameter and Urbach energy E_u with carbon fraction x .

These parameters saturate at $B \sim 250 \text{ cm}^{-1/2} \text{ eV}^{-1/2}$ and $E_u \sim 420 \text{ meV}$ in C-rich a -Si_{1-x}C_x:H, which are values typical of a -C:H films.^{26,27}

Room-temperature PL is not seen in the Si-rich films. For a -Si:H, the PL is attributed to tail-to-tail states recombination of localized electron-hole pairs (EHPs). This radiative mechanism is normally detected only under low-temperature measurement. It is quenched at higher temperature ($>100 \text{ K}$) because the carrier mobilities are enhanced, resulting in more nonradiative recombinations through paramagnetic Si dangling bond states. The rate of this phonon-assisted recombination is about 10 orders of magnitude higher than that of the band tail radiative recombination, therefore the PL is easily quenched by the presence of a few nonradiative recombination centers.¹⁶ As our Si-rich a -Si_{1-x}C_x:H have a microstructure similar to that of a -Si:H, thermal quenching is likely the reason that accounts for the absence of room-temperature PL.²⁸ In C-rich a -Si_{1-x}C_x:H, room-temperature PL is observed, as shown in Fig. 6. The microstructures of these films resemble that of a -C:H, as evidenced from the discussions so far. Therefore, the PL mechanism of these C-rich a -Si_{1-x}C_x:H can be interpreted using the framework of a -C:H, which attributes it to the radiative recombination of photoexcited EHPs in sp^2 bonded clusters. The π - π^* gap in sp^2 sites are much narrower than the σ - σ^* gap, and the latter acts as a barrier that strongly localizes the π - π^* band edge states. Therefore, the EHPs are closely correlated by Coulomb interaction and display a short lifetime. Correspondingly, the PL has a strong polarization memory, is not quenched by the electric field and can be observed at room temperature.²⁷ Since the samples exhibit similar E_u and the excitation energy ($\sim 3.41 \text{ eV}$) is higher than their optical gaps, we would expect the PL peak energy (E_{PL}) to be correlated to the E_{04} gap, as a result of the thermalization of the carriers at the band edges.²⁷ Indeed, a linear relation exists, as can be seen in the inset of Fig. 6. The result is contrary to that obtained by Conde *et al.*²⁵ for their ECR-CVD grown a -Si_{1-x}C_x:H under low microwave power (150 W), where a constant PL peak at 2.35 eV was found, independent of E_{04} .²⁵ The full width at half maximum (FWHM) of the PL band for the three samples are

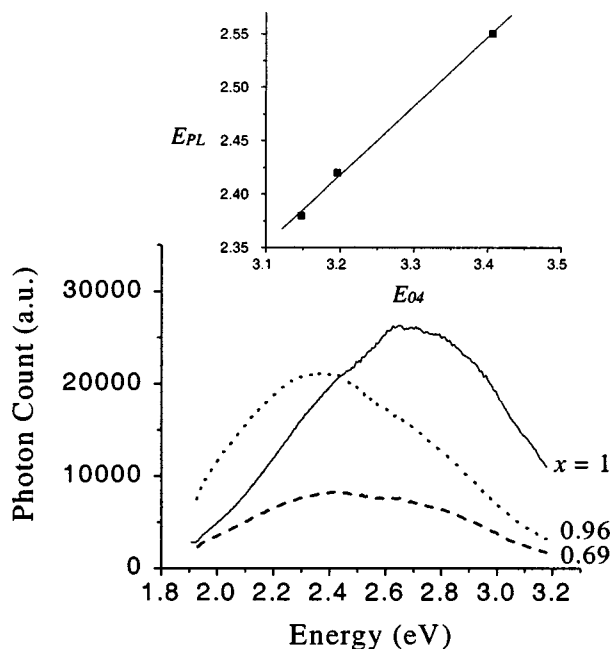


FIG. 6. The room-temperature PL of carbon-rich $a\text{-Si}_{1-x}\text{C}_x\text{:H}$. Inset: the linear relation observed between the PL peak energy (E_{PL}) and the E_{04} gap.

found to be almost constant at 0.9 eV, attributed to the nearly constant E_u of these samples. We have further found that the $\text{FWHM} \approx 2.14 E_u$, and the proportional constant is similar to that obtained in our earlier study of ECR-CVD grown C-rich $a\text{-Si}_{1-x}\text{C}_x\text{:H}$.⁶ These results support that the PL broadening is attributed to the disorder broadening arising from the broad band tails.⁶

IV. CONCLUSION

The optical and structural properties of $a\text{-Si}_{1-x}\text{C}_x\text{:H}$ over a wide range of C fraction x are investigated. There is a higher degree of disorder in the microstructure at increasing x , as shown by the evolution of the Tauc B parameter and Urbach energy E_u . The Raman and FTIR spectra reveal the presence of Si—C bonds at intermediate x , and an increase in the sp^3 C—C bonds with increasing x for the C-rich films. These are attributed to the high microwave power applied and the strong H_2 dilution in the gas mixture. The optical gap increases with carbon incorporation and is nearly saturated at large x , due to the enhanced sp^3 C—C bonding. Blue PL is achieved at room temperature for the C-rich $a\text{-Si}_{1-x}\text{C}_x\text{:H}$, owing to the high optical gap of the films. The PL peak

energies are correlated to the optical gap, and the FWHM to the Urbach energy E_u . From these results, it is deduced that the broadening of the band tail states contributes to the shape of the PL spectra observed.

- ¹R. Platz, D. Fischer, and A. Shah, *Amorphous Silicon Technology 1992* (Material Research Society, Pittsburgh, 1992); Mater. Res. Soc. Symp. Proc. **258**, 923 (1995).
- ²H. Kukimoto, *Amorphous Light-Emitting Devices*, Semiconductors and Semimetals Vol. 21D, edited by J. I. Pankove (Academic, Press Florida, 1984), Chap. 12.
- ³P. G. LeComber, *J. Non-Cryst. Solids* **115**, 1 (1989).
- ⁴R. Nozawa, H. Takeda, M. Ito, M. Hori, and T. Goto, *J. Appl. Phys.* **85**, 1172 (1999).
- ⁵Rusli, S. F. Yoon, H. Yang, Q. Zhang, J. Ahn, and Y. L. Fu, *J. Vac. Sci. Technol. A* **16**, 572 (1998).
- ⁶J. Cui, Rusli, S. F. Yoon, M. B. Yu, K. Chew, J. Ahn, and Q. Zhang, *J. Appl. Phys.* **89**, 2699 (2001).
- ⁷A. Desalvo, F. Giorgis, C. F. Pirri, E. Tresso, P. Rava, R. Gallani, R. Rizzoli, and C. Summone, *J. Appl. Phys.* **81**, 7973 (1997).
- ⁸F. Alvarez, M. Sebastiani, F. Pozzilli, P. Fiorini, and F. Evangelisti, *J. Appl. Phys.* **71**, 267 (1992).
- ⁹N. M. Amer and W. B. Jackson, in *Semiconductors and Semimetals*, Vol. 21B, edited by J. I. Pankove (Academic, Florida, 1984), Chap. 3.
- ¹⁰I. Pereyra, M. N. P. Carreno, M. H. Taboaniks, R. J. Prado, and M. C. A. Fantini, *J. Appl. Phys.* **84**, 2371 (1998).
- ¹¹R. A. C. M. van Swaaij, A. J. M. Berntsen, W. G. J. H. M. van Sark, H. Herremans, J. Bezemer, and W. F. van der Weg, *J. Appl. Phys.* **76**, 251 (1994).
- ¹²M. A. El Khakani, D. Guay, M. Chaker, and X. H. Feng, *Phys. Rev. B* **51**, 4903 (1995).
- ¹³V. Chu, J. P. Conde, J. Jarego, P. Brogueira, J. Rodriguez, N. Banadas, and J. C. Soares, *J. Appl. Phys.* **78**, 3164 (1995).
- ¹⁴Y. Katayama, D. Kruangam, and T. Shimada, *Philos. Mag. B* **43**, 283 (1981).
- ¹⁵S. Z. Han, H. M. Lee, and H.-S. Kwon, *J. Non-Cryst. Solids* **170**, 201 (1994).
- ¹⁶R. A. Street, *Hydrogenated Amorphous Silicon* (Cambridge University Press, Great Britain, 1991).
- ¹⁷M. Katiyar, Y. H. Yang, and J. R. Abelson, *J. Appl. Phys.* **78**, 1659 (1995).
- ¹⁸M. A. Petrich, K. K. Gleason, and J. A. Reimer, *Phys. Rev. B* **36**, 9722 (1987).
- ¹⁹M. A. Tamor and W. C. Vassell, *J. Appl. Phys.* **76**, 3823 (1994).
- ²⁰A. C. Ferrari and J. Robertson, *Phys. Rev. B* **61**, 14095 (2000).
- ²¹S. F. Yoon, R. Ji, and J. Ahn, *Philos. Mag.* **77**, 197 (1998).
- ²²K. W. R. Gilkes, S. Praver, K. W. Nugent, J. Robertson, H. S. Sands, Y. Lifshitz, and X. Shi, *J. Appl. Phys.* **87**, 7283 (2000).
- ²³J. Robertson, *Philos. Mag. B* **66**, 615 (1992).
- ²⁴J. Bullot, M. Gauthier, M. Schmidt, Y. Catherine, and A. Zamouche, *Philos. Mag. B* **49**, 489 (1984).
- ²⁵J. P. Conde, V. Chu, M. F. da Silva, S. Arekat, A. Fedorov, M. N. Berberan-Santos, F. Giorgis, and C. F. Pirri, *J. Appl. Phys.* **85**, 3327 (1999).
- ²⁶J. C. Angus, P. Koidl, and S. Domitz, in *Plasma Deposited Thin Films*, edited by J. Mort and F. Jansen (CRC Press, Florida, 1986), Chap. 4.
- ²⁷Rusli, J. Robertson and G. A. J. Amarantunga, *J. Appl. Phys.* **80**, 2998 (1996).
- ²⁸L. R. Tessler and I. Solomon, *Phys. Rev. B* **52**, 10962 (1995).